Hindawi
International Journal of Antennas and Propagation
Volume 2023, Article ID 9359671, 10 pages
https://doi.org/10.1155/2023/9359671

Research Article

A Compact Broad Circularly Polarized Cross-Dipole Antenna with Grounded Parasitic Elements

Dong Yang,[1] Lichao Hao,[1] and Lei Wang[2]

[1]*Zhengzhou Key Laboratory of Electronic Information Functional Materials and Devices, Faculty of Engineering, Huanghe Science and Technology College, Zhengzhou, Henan, China*
[2]*Science and Technology on Reliability Physics and Application of Electronic Component Laboratory, CEPREI, Guangzhou, China*

Correspondence should be addressed to Lei Wang; leiwang@ceprei.com

Received 23 July 2023; Revised 20 August 2023; Accepted 7 September 2023; Published 21 September 2023

Academic Editor: Rajkishor Kumar

A new wideband cross-dipole antenna (CDA) with a circularly polarized (CP) characteristic is proposed in this article. The antenna consists of four L-shaped patches, two modified trapezoid-microstrip lines as an impedance tuner, a pair of vacant-quarter feeding loops as a continuous-phase feeding network, and four grounded inverted L-shaped strips as parasitic elements. It is noticed that the grounded inverted L-shaped strips are inserted directly below the L-shaped patches to increase the CP bandwidth and enhance the gains of the antenna, which is different from the conventional parasitic elements. First, a pair of vacant-quarter feeding loops is used as a feeding structure to provide a sequential phase characteristic. Second, four L-shaped patches as driven elements are connected to the feeding structure to excite two CP resonant modes. Third, two modified trapezoid-microstrip lines are inserted into the feeding structure to adjust the impedance match. Moreover, four grounded inverted L-shaped strips are introduced into the square reflector to achieve wider CP operation by utilizing a gap capacitive coupling feeding way. Finally, the proposed antenna is simulated, manufactured, and measured to verify the design rationality. The measured results indicate the proposed antenna has a broad 3-dB ARBW of 82.5% (1.38–3.32 GHz, 2.35 GHz) and a wide −10-dB IBW of 81.2% (1.18–3.04 GHz, 2.29 GHz). Furthermore, the measured and simulated CP bandwidths are 75.1% (1.38–3.04 GHz, 2.21 GHz) and 74.7% (1.36–2.98 GHz, 2.17 GHz), which is suitable for CP applications in WiBro (2.3–2.39 GHz) and GPS (L1 1.575 GHz) bands.

1. Introduction

Cross-dipole antennas (CDAs) are becoming more and more popular in many communication systems because of their outstanding features of wide bandwidth, directional radiation, and flexible structure. In addition, circularly polarized (CP) CDA has attracted a lot of attention in the communication system as one of the potential candidates, compared with the linearly polarized CDA. This is because that the CP MDA has obvious advantages in reducing polarization misalignment and alleviating multipath interference.

Recently, a pair of orthogonal vacant-quarter printed rings as a continuous rotating feeding structure, which could stimulate two kinds of signals with equal amplitude and phase a difference of 90 degrees, is massively used in to the CP CDAs. Generally, these CP CDAs with continuous rotating feeding structures could be categorized into modified CP CDAs and CP CDAs with parasitic elements. First, in order to achieve wideband 3-dB axial ratio bandwidth (ARBW), various different shapes of CDAs are designed in [1–7]. These modified CDAs include the liner strip (15.6%) [1], rectangular strip (27%) [2], stepped rectangular patches (55.1%) [3], L-shaped patch (67.5%) [4], triangular bowtie dipoles (39.0%) [5], slit-loaded rectangular patch (23.2%) [6], and asymmetric bowtie patch (51%) [7]. Second, many parasitic elements are inserted into the CP CDAs to obtain wide CP bandwidths in [8–22]. This is because that these parasitic elements can stimulate an additional CP resonant

mode and participate in the radiation of the CDA. Similarly, these parasitic elements consist of a folded ground plane (74.7%) [8], slot-etched rectangular patches (72.7%) [9], a stepped cross-dipole (59.1%) [10], additional square-patches (66%) [11], asymmetric L-shaped strips (52.2%) [12], triangle patches (58.9%) [13], shorted coupled pads (85.5%) [14], four rotated metallic plates (106.1%) [15], a slot-bowtie cross-dipole (90.9%) [16], a trapezoidal dipole (63.4%) [17], a half-ellipse dipole (68.6%) [18], asymmetric cross-loop (53.4%) [19], dual-square cavity ground (66.7%) [20], parasitic composite cavity (96.6%) [21], rotated-circular dipoles (47.8%) [22], and magneto-electric dipoles (47.7%) [23].

Based on the concept of paganism, a new CD CPA with four grounded inverted L-shaped strips is proposed in this work. It is noticed that the grounded inverted L-shaped strips are inserted directly below the L-shaped patches to increase the CP bandwidth and enhance the gains of the antenna, which is different from the conventional parasitic elements. The CD CPA is composed of four L-shaped patches, two modified trapezoid-microstrip lines as an impedance tuner, a pair of vacant-quarter feeding loops as a continuous-phase feeding network, and four grounded inverted L-shaped strips as parasitic elements. First, a pair of vacant-quarter feeding loops is used as a feeding structure to provide a sequential phase characteristic. Second, four L-shaped patches as driven elements are connected to the feeding structure to excite two CP resonant modes. Third, two modified trapezoid-microstrip lines are inserted into the feeding structure to adjust the impedance match. Moreover, four grounded inverted L-shaped strips are introduced into the square reflector to achieve wider CP operation by utilizing a gap capacitive coupling feeding way. Finally, the proposed antenna is simulated, manufactured, and measured to verify the design rationality.

2. Antenna Design

2.1. Antenna Configuration. The structure and dimensions of the CD CPA are depicted in Figure 1 and Table 1, respectively. As seen, the presented CD CPA includes four L-shaped patches ($L3 \times W3$ and $L4 \times W4$) as driven elements, two modified trapezoid-microstrip lines ($L1 \times W1$ and $L2 \times W2$) as an impedance tuner, a pair of vacant-quarter feeding loops ($R0 \times R1$) as a continuous-phase feeding network, a square ground plane ($L \times W$) as a reflector, and four grounded inverted L-shaped strips ($L5 \times W5$) with a height of $h2$ as parasitic elements. The CD CPA is printed at a Rogers. RT substrates ($\varepsilon r = 4.4$, $\tan \delta = 0.02$) with a height of $h1$. Note that vacant-quarter feeding loops with the length of $\sim\lambda_g/4$ (λ_g is the guided wavelength at the center frequency) are used to provide a 270° phase difference, which can stimulate a CP operation mode [15]. The outer and outer radii of the strip are $R0$ and $R1$, respectively. In addition, four grounded inverted L-shaped strips are etched into the square ground plane to excite a CP resonant mode. The optimized dimensions of the designed antenna are conducted through utilizing high-frequency electromagnetic simulator (ANSYS HFSS), and the optimal parameter values are summarized in Table 1.

2.2. Step-by-Step Design Process. Figure 2 plots four step-by-step prototypes (Ant. I, II, III, and proposed antenna) as a comparison to explain the working mechanism of the CD CPA. The corresponding −10-dB return loss, and 3-dB AR are together depicted in Figures 3(a) and 3(b), respectively. As seen, Ant. 1 has a pair of vacant-quarter feeding loops with four L-shaped patches, which could excite multiple CP resonant modes near 2.1 GHz. However, the return loss of Ant. I is not good due to the poor impedance match. In order to improve the impedance match, two modified trapezoid-microstrip lines as an impedance tuner are introduced into the Ant. II. As seen, compared with the results of Ant. I, the IBW of Ant. II can be significantly improved, and the ARs are not obviously changed. Note that the ARBW of Ant. II cannot completely cover the IBW of that. Therefore, four grounded parasitic I-shaped and L-shaped strips are inserted into the Ant. III and the proposed antenna to expend the ARBW, respectively. It is observed that the ARBWs of Ant. III and the proposed antenna could be obviously improved compared with the ARBW of Ant. II. In addition, the IBW and ARBW of the proposed antenna are the best. This is because that the parasitic L-shaped strips can stimulate an additional CP resonant mode at high frequencies. As a result, the proposed CD CPA features a wide 10-dB IBW of 83.8% (2.1 GHz, 1.22–2.98 GHz) and a 3-dB ARBW of 81.7% (2.3 GHz, 1.36–3.24 GHz). In addition, a comparison of the proposed CD CPA with previously reported antennas is depicted in Table 2, which reveals that the antenna has a wider CP performance.

2.3. Simulated Surface Current Analysis. For the purpose of revealing the CP operating principle, the vector surface-current distributions on the designed CP CDA at 1.85 and 2.8 GHz are plotted in Figure 4. Note that the vector surface currents of the grounded L-shaped strips are also depicted in Figure 4 for explaining the role of the parasitic L-shaped strips. Based on Figure 4, it is observed that the vector surface current is mainly distributed on the L-shaped patches, and a small amount is distributed on the grounded L-shaped strips. In addition, it is noticed that the surface currents of the grounded L-shaped strip are always opposite to that of the L-shaped patches, which means the total surface currents are reduced. It is well known that the smaller the surface current, the higher the operating frequency. In addition, compared with the surface currents of the parasitic L-shaped strip at 1.85 and 2.8 GHz, it is found that the surface currents at 2.8 GHz are greater than those at 1.85 GHz. Therefore, the working frequency of the antenna shifts toward high frequency. Finally, with the change of phase at 0° and 90°, the direction of the surface-current on the CP CDA begins to rotate clockwise at 1.85 and 2.8 GHz, which means the CP CDA could radiate the left-hand CP waves in $+z$ direction.

2.4. Antenna Parameter Analysis. To reveal the influence of the antenna's dimensions on its CP characteristics, multiple parameter scans are conducted through changing the relevant antenna's sizes, which include the side length ($L2$) of the

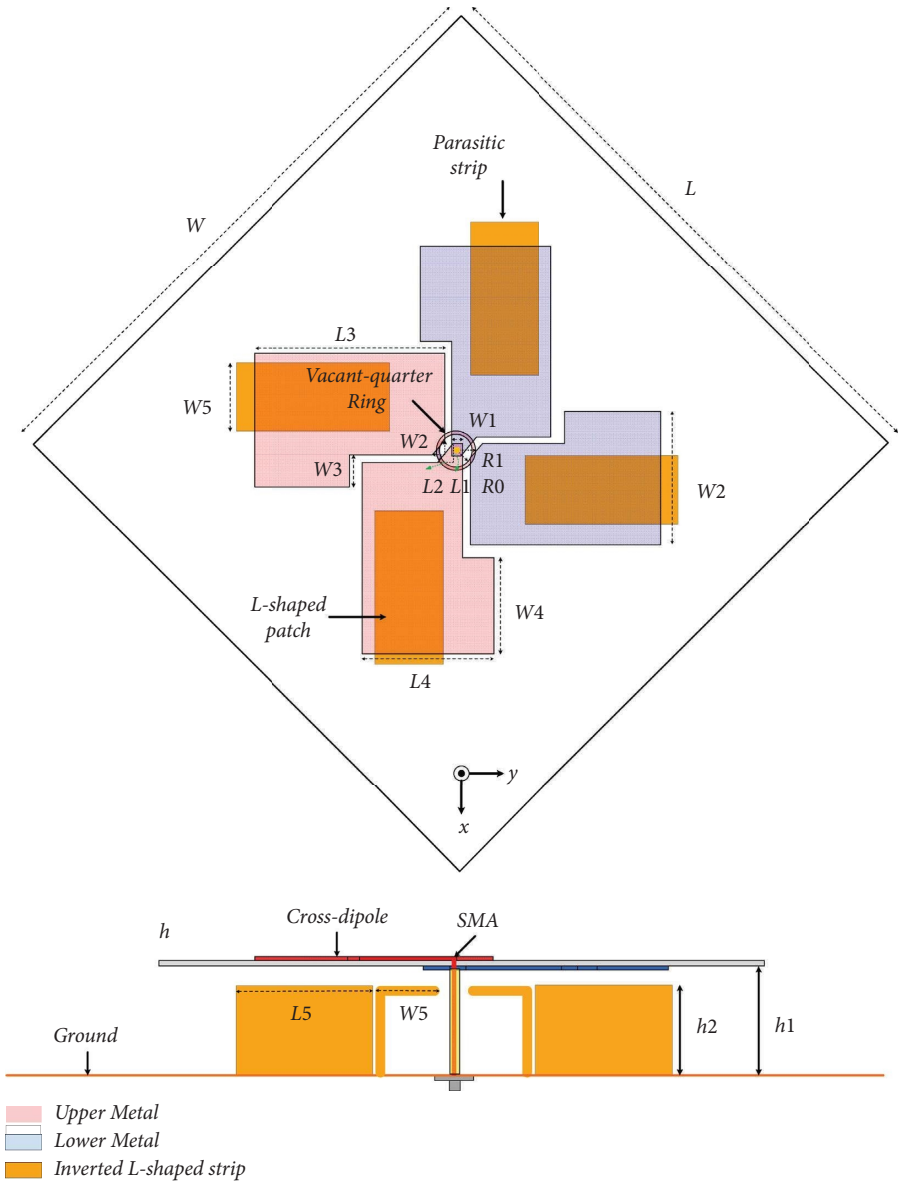

Figure 1: Geometry of the CD CPA.

modified trapezoid-microstrip lines, the side length ($L4$) of the L-shaped patches, and the length ($L5$) and height ($h2$) of the grounded L-shaped strips. The corresponding return loss and AR values are plotted in Figure 5. Multiple interesting phenomena can be discovered. One is that the side length ($L2$) of the modified trapezoid-microstrip lines has a significant influence on the IBW due to the impedance tuning impact. The second is that the side length ($L4$) of the L-shaped patches has obviously an impact on the IBW and ARBW, as the L-shaped patches are the main driving element. The third is that the length ($L5$) and height ($h2$) of the grounded L-shaped strips as parasitic elements simultaneously determine the IBW and ARBW at high frequencies. This is because that ground L-shaped strips play a key role in stimulating an additional CP resonant mode at high frequencies, which is consistent with the above results of the step-by-step design process. Finally, when the parameters $L2 = 4.2$ mm, $L4 = 36$ mm, $L5 = 46$ mm, and $h2 = 30$ mm, the optimal IBW and ARBW could be achieved.

3. Experimental Results

To prove the rationality of the design, an optimal antenna model was printed and measured in this subsection. The CP CDA's model was simulated, manufactured, and tested. The vector network analyzer (ZNB 20) and the Satimo Starlab system are applied to measure the return loss |S11|, ARs, gains, and radiation pattern values. The comparisons between the simulated and tested results are plotted in Figures 6–8. As seen, the simulated and tested return loss

Table 1: Key parameters of the CD CPA (unit: mm).

Sizes	Values
L	180
$R0$	4.7
$L1$	4.8
$L2$	4.2
$L3$	52
$L4$	36
$L5$	46
h	0.8
$h2$	30
W	180
$R1$	5.2
$W1$	2.8
$W2$	3.6
$W3$	8.6
$W4$	26
$W5$	20
$h1$	36.6

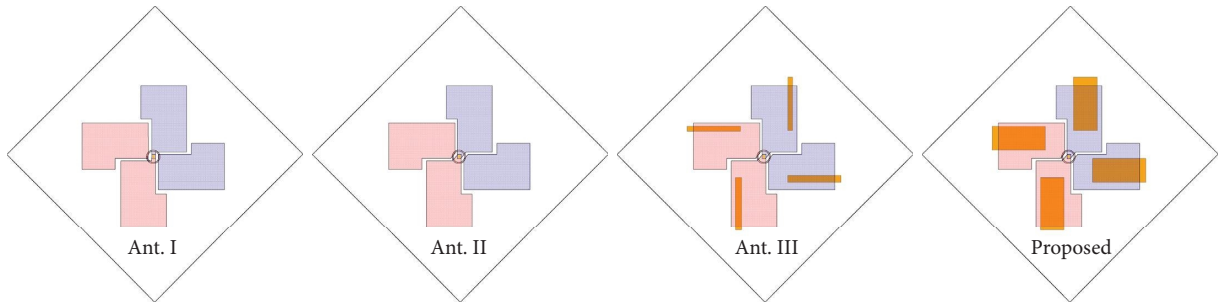

Figure 2: Five antenna models in the design process.

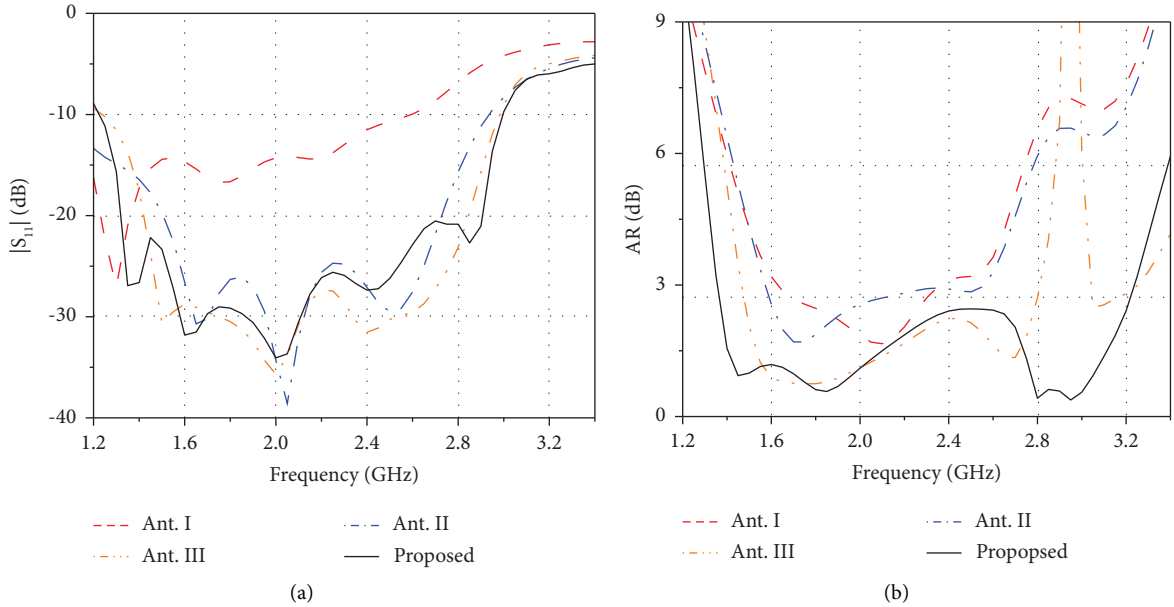

Figure 3: $|S_{11}|$, AR, and gain curves for different antennas: (a) $|S_{11}|$ curves and (b) AR curves.

and AR values versus frequency are depicted in Figures 6(a) and 6(b), respectively. It is observed that the measured 3-dB ARBW and −10-dB IBW are 82.5% (1.38–3.32 GHz, 2.35 GHz) and 81.2% (1.18–3.04 GHz, 2.29 GHz), while the simulated results are 81.7% (1.36–3.24 GHz, 2.3 GHz) and 83.8% (1.22–2.98 GHz, 2.1 GHz). Furthermore, the

Table 2: Comparison of the proposed antenna to previously reported antennas.

Ref. antenna	Antenna size (λ_0)	−10-dB IBW (%)	3-dB ARBW (%)	CP-BW (%)
[3]	$2.06 \times 2.06 \times 0.13$	66.9	55.1	55.1
[4]	$1.81 \times 1.81 \times 0.23$	92.8	67.5	67.5
[5]	$2.06 \times 2.06 \times 0.26$	57.6	39.0	39.0
[6]	$0.44 \times 0.44 \times 0.14$	31.6	23.2	23.2
[7]	$0.88 \times 0.88 \times 0.23$	57.0	51.0	51.0
[8]	$1.08 \times 1.08 \times 0.26$	85.7	100	74.7
[9]	$1.11 \times 1.11 \times 0.28$	99.2	72.7	72.7
[10]	$1.12 \times 1.12 \times 0.24$	80.8	59.1	59.1
[11]	$1.04 \times 1.04 \times 0.26$	77.6	66.0	66
[12]	$1.03 \times 1.03 \times 0.25$	100	52.2	52.2
[14]	$1.17 \times 1.17 \times 0.29$	95.0	85.5	85.5
[15]	$0.28 \times 0.28 \times 0.11$	115.6	106.1	106.1
[17]	$0.46 \times 0.46 \times 0.10$	78.3	63.4	63.4
[18]	$0.97 \times 0.97 \times 0.32$	82	68.6	68.6
[19]	$1.10 \times 1.10 \times 0.28$	67.5	53.4	53.4
[20]	$0.57 \times 0.57 \times 0.24$	79.4	66.7	66.7
[21]	$0.71 \times 0.71 \times 0.35$	106	96.6	96.6
[22]	$0.40 \times 0.40 \times 0.17$	66.2	47.8	47.8
[23]	$1.10 \times 1.10 \times 0.29$	73.3	47.7	47.7
Proposed	$1.08 \times 1.08 \times 0.26$	81.2	82.5	74.7

λ_0 is the centre frequency of CP bandwidth.

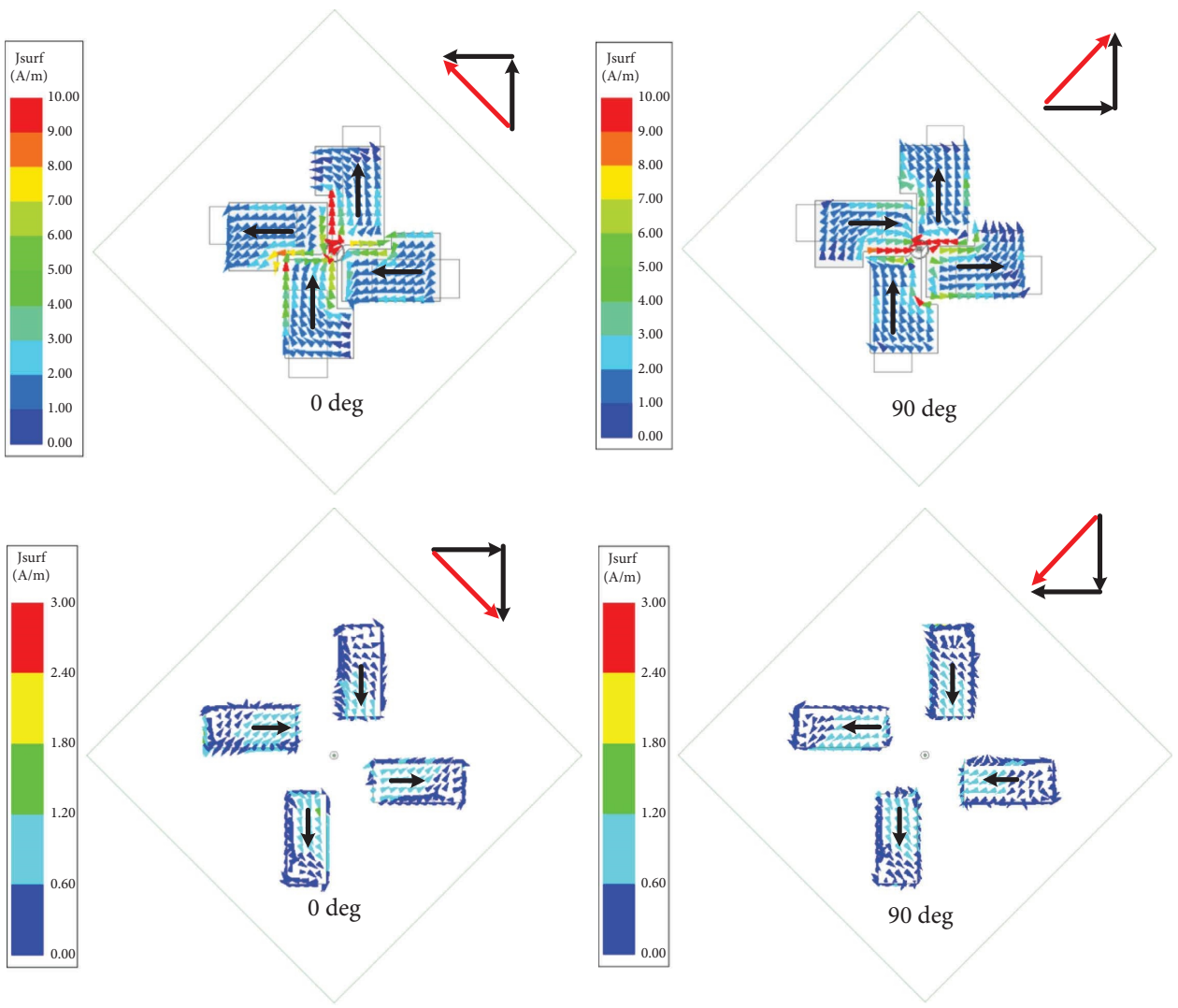

(a)

Figure 4: Continued.

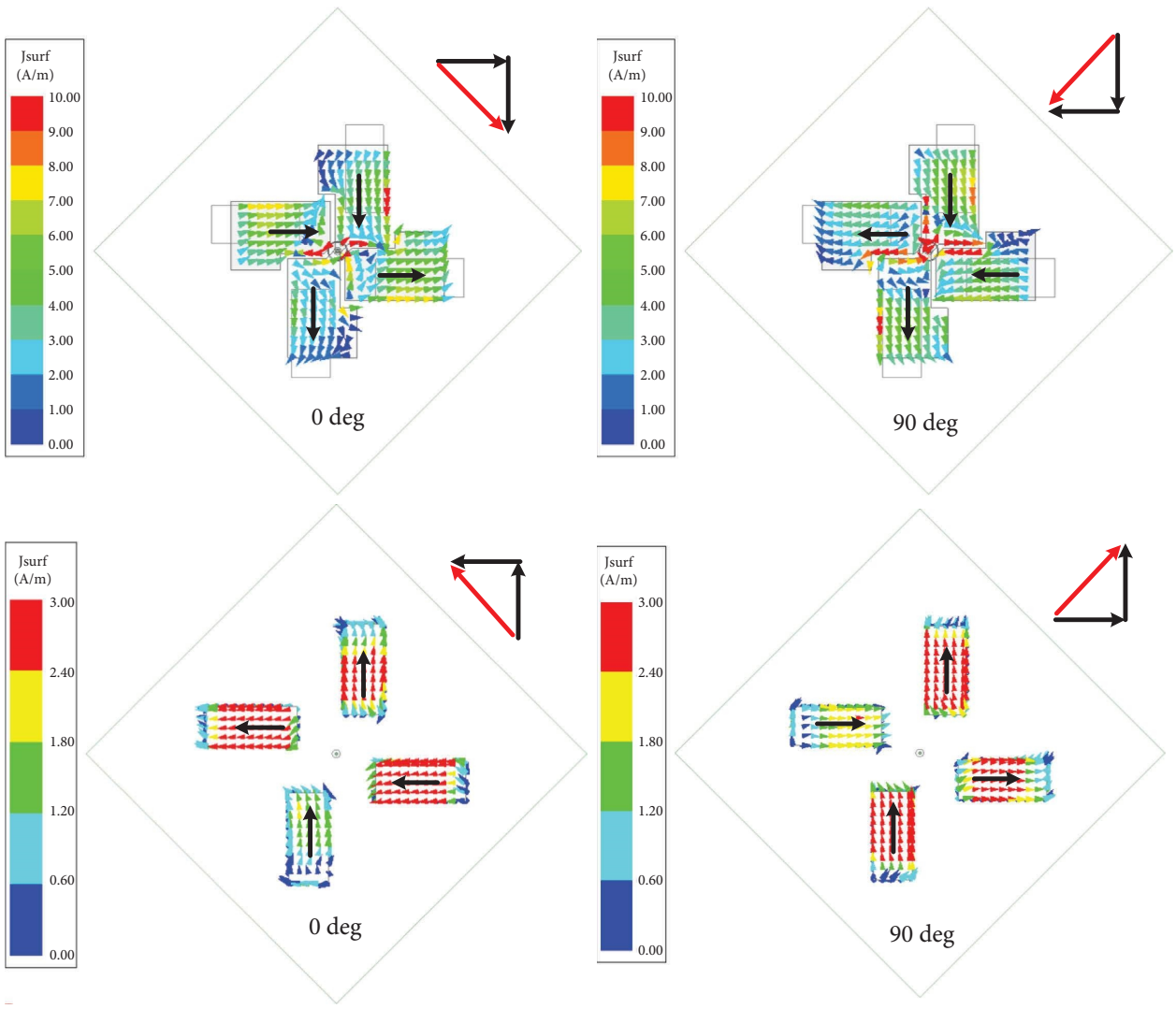

(b)

Figure 4: Simulated current distributions on the CP CDA with different phases at (a) 1.85 GHz and (b) 2.8 GHz, respectively.

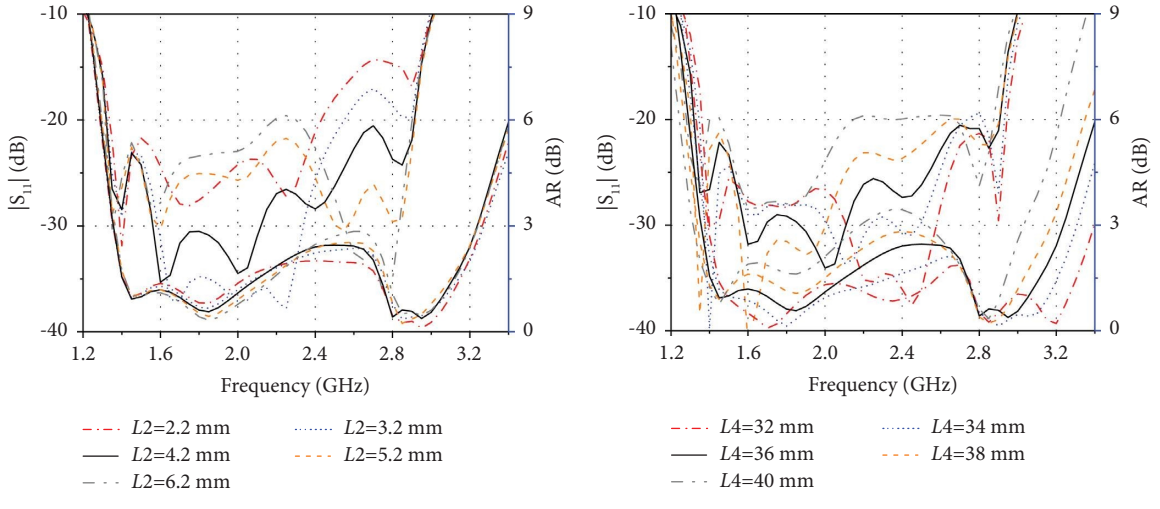

(a) (b)

Figure 5: Continued.

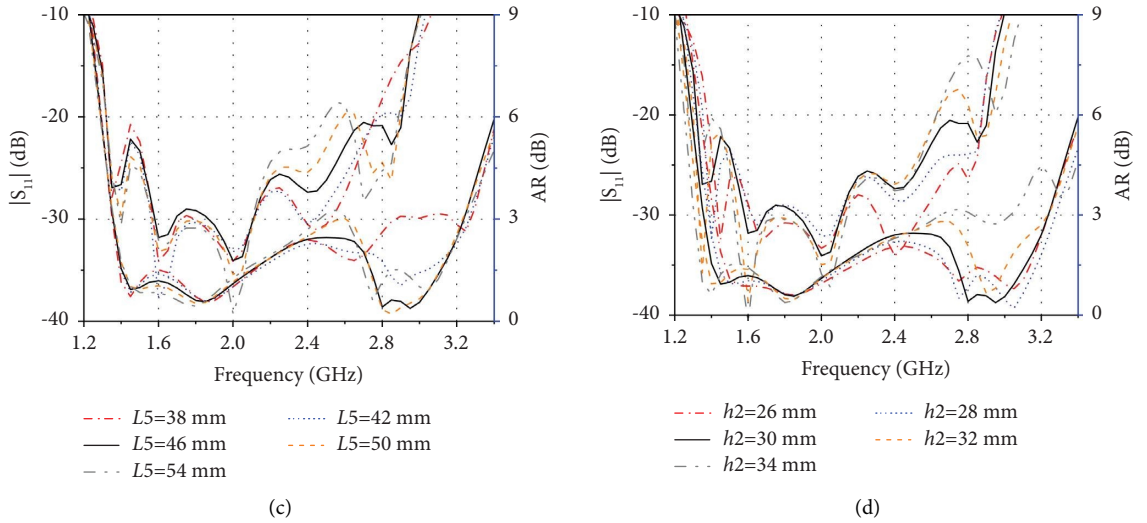

Figure 5: $|S_{11}|$ and AR curves of the designed antenna with different parameters: (a) $L2$, (b) $L4$, (c) $L5$, and (d) $h2$.

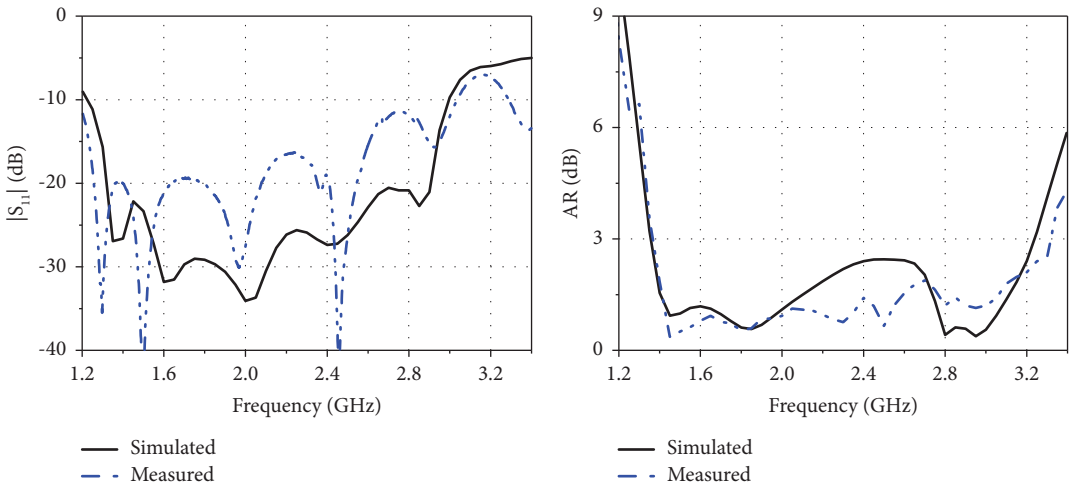

Figure 6: Simulated and measured $|S_{11}|$ and AR results of CP CDA.

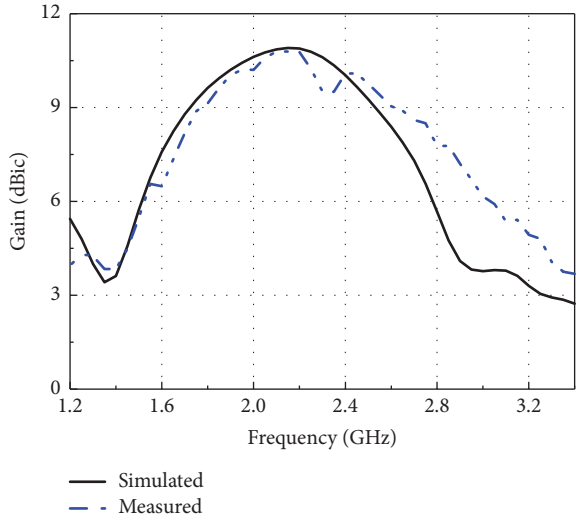

Figure 7: Continued.

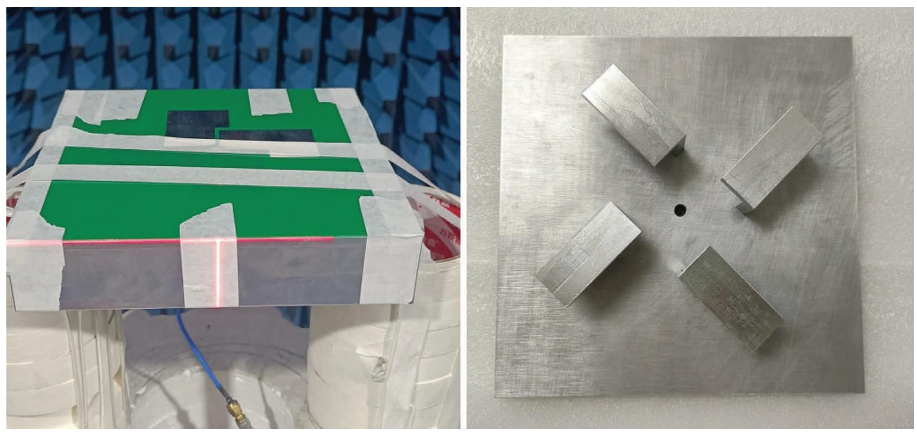

(b)

Figure 7: Simulated and tested antenna gains and measurement photograph: (a) gain curves and (b) photograph.

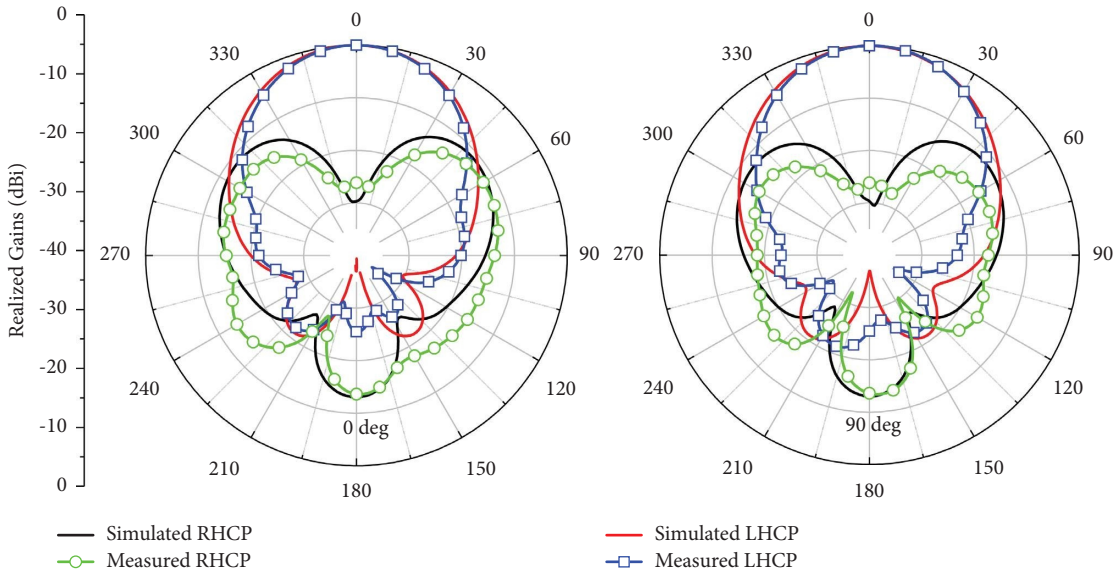

(a)

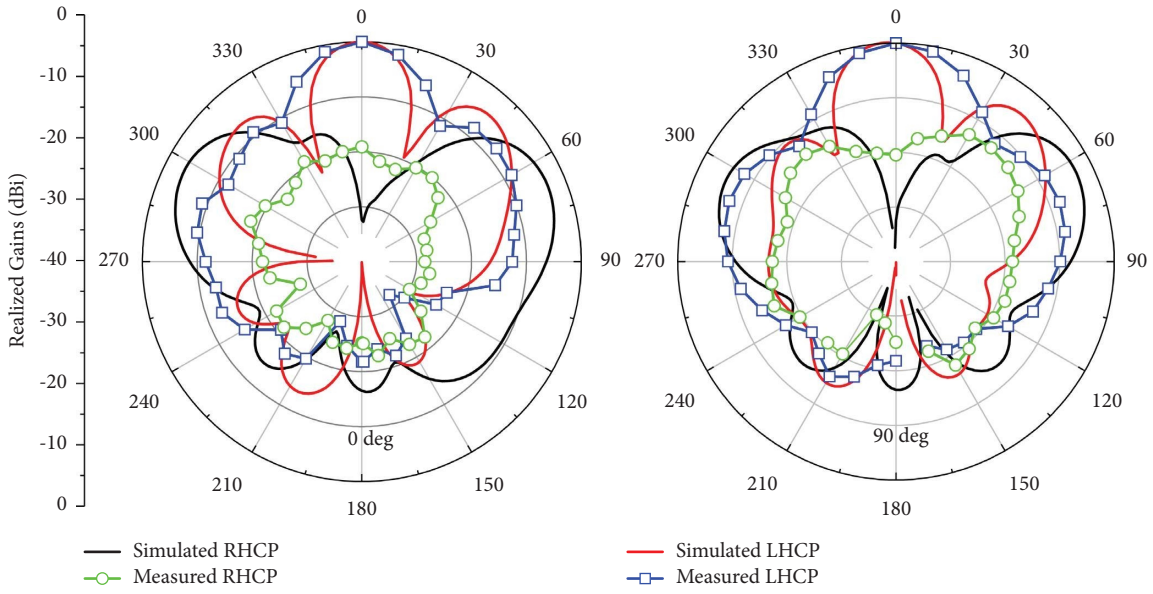

(b)

Figure 8: Simulated and tested radiation patterns of the CP CDA antenna at: (a) 1.85 GHz and (b) 2.8 GHz.

measured and simulated overlapped CP bandwidths are 75.1% (1.38–3.04 GHz, 2.21 GHz) and 74.7% (1.36–2.98 GHz, 2.17 GHz). Besides, the simulated and measured realized gains and measurement photograph of the designed antenna are also shown in Figures 7(a) and 7(b). The measured peck gain is 10.8 dBic at 2.15 GHz. Eventually, the simulated and measured normalized radiation patterns with the E-plane and H-plane at 1.85 and 2.80 GHz are depicted in Figure 8. As depicted, the right-hand CP waves are weaker than the left-hand CP parts by more than 20-dB, which shows the designed antenna could radiate the left-hand CP wave in the $+z$ direction. Although a slight discrepancy between the tested and simulated results could be found, in general, these results have been able to demonstrate the rationality of the design.

4. Conclusions

A new wideband cross-dipole antenna (CDA) with a circularly polarized (CP) characteristic is proposed in this article. The antenna consists of four L-shaped patches, two modified trapezoid-microstrip lines as an impedance tuner, a pair of vacant-quarter feeding loops as a continuous-phase feeding network, and four grounded inverted L-shaped strips as parasitic elements. It is noticed that the grounded inverted L-shaped strips are inserted directly below the L-shaped patches to increase the CP bandwidth and enhance the gains of the antenna, which is different from the conventional parasitic elements. First, a pair of vacant-quarter feeding loops is used as a feeding structure to provide a sequential phase characteristic. Second, four L-shaped patches as driven elements are connected to the feeding structure to excite two CP resonant modes. Third, two modified trapezoid-microstrip lines are inserted into the feeding structure to adjust the impedance match. Moreover, four grounded inverted L-shaped strips are introduced into the square reflector to achieve wider CP operation by utilizing a gap capacitive coupling feeding way. Finally, the proposed antenna is simulated, manufactured, and measured to verify the design rationality. The measured results indicate the proposed antenna has a broad 3-dB ARBW of 82.5% (1.38–3.32 GHz, 2.35 GHz) and a wide −10-dB IBW of 81.2% (1.18–3.04 GHz, 2.29 GHz). Furthermore, the measured and simulated CP bandwidths are 75.1% (1.38–3.04 GHz, 2.21 GHz) and 74.7% (1.36–2.98 GHz, 2.17 GHz), which is suitable for CP applications in WiBro (2.3–2.39 GHz) and GPS (L1 1.575 GHz) bands.

Data Availability

The data that support the findings of this study are available from the corresponding authors upon reasonable request.

Conflicts of Interest

The authors declare that they have no conflicts of interest.

Acknowledgments

This research was funded by Zhengzhou Key Laboratory of Electronic Information Functional Materials and Devices (121PYFZX178); Zhengzhou Key Laboratory of Intelligent Measurement Techniques and Applications (201791); cooperative education project of the Ministry of Education (20180233002); and cooperative education project of the Ministry of Education (202002179007).

References

[1] J.-W. Baik, K.-J. Lee, W.-S. Yoon, T.-H. Lee, and Y.-S. Kim, "Circularly polarised printed crossed dipole antennas with broadband axial ratio," *Electronics Letters*, vol. 44, no. 13, pp. 785-786, 2008.

[2] Y. He, W. He, and H. Wong, "A wideband circularly polarized cross-dipole antenna," *IEEE Antennas and Wireless Propagation Letters*, vol. 13, pp. 67–70, 2014.

[3] W. Yang, Y. Pan, S. Zheng, and P. Hu, "A low-profile wideband circularly polarized crossed-dipole antenna," *IEEE Antennas and Wireless Propagation Letters*, vol. 16, pp. 2126–2129, 2017.

[4] X. Liang, J. Ren, L. Zhang et al., "Wideband circularly-polarized antenna with dual-mode operation," *IEEE Antennas and Wireless Propagation Letters*, vol. 18, no. 4, pp. 767–770, 2019.

[5] S.-W. Qu, C. H. Chan, and Q. Xue, "Wideband and high-gain composite cavity-backed crossed triangular bowtie dipoles for circularly polarized radiation," *IEEE Transactions on Antennas and Propagation*, vol. 58, no. 10, pp. 3157–3164, 2010.

[6] Q. Chen, H. Zhang, L. Yang, and T. Zhong, "A metasurface-based slit-loaded wideband circularly polarized crossed dipole antenna," *International Journal of RF and Microwave Computer-Aided Engineering*, vol. 28, no. 1, Article ID e21173, 2018.

[7] H. H. Tran and I. Park, "Wideband circularly polarized cavity-backed asymmetric crossed bowtie dipole antenna," *IEEE Antennas and Wireless Propagation Letters*, vol. 15, pp. 358–361, 2016.

[8] L. Wang, K. Chen, Q. Huang et al., "Wideband circularly polarized cross-dipole Antenna with folded ground plane," *IET Microwaves, Antennas & Propagation*, vol. 15, no. 5, pp. 451–456, 2021.

[9] Z. Zhao, Y. Li, M. Xue, L. Wang, Z. Tang, and Y. Yin, "Design of wideband circularly polarized crossed-dipole antenna using parasitic modified patches," *IEEE Access*, vol. 7, pp. 75227–75234, 2019.

[10] G. Feng, L. Chen, X. Xue, N. Li, and X. Shi, "Broadband CP crossed-stepped-dipole antenna incorporating a cross slotted square patch," *IET Microwaves, Antennas & Propagation*, vol. 13, no. 3, pp. 340–345, 2019.

[11] L. Wang, W.-X. Fang, Y. F. En, Y. Huang, W.-H. Shao, and B. Yao, "Wideband circularly polarized cross-dipole antenna with parasitic elements," *IEEE Access*, vol. 7, pp. 35097–35102, 2019.

[12] S.-M. Liao, G.-L. Huang, W. He, X.-C. Chen, and T. Yuan, "A wideband circularly polarized cross-dipole antenna with two asymmetric L-shaped strips," in *Proceedings of the 2019 International Conference On Microwave And Millimeter Wave Technology (ICMMT)*, Guangzhou, China, May 2019.

[13] H. H. Tran, N. Nguyen-Trong, T. K. Nguyen, and A. M. Abbosh, "Bandwidth enhancement utilizing bias circuit as parasitic elements in a reconfigurable circularly polarized antenna," *IEEE Antennas and Wireless Propagation Letters*, vol. 17, no. 8, pp. 1533–1537, 2018.

[14] Z. Zhao, Y. Li, L. Wang, Z. Tang, and Y. Yin, "Design of broadband circularly polarized antenna via loading coupled

rotated dipoles," *Microwave and Optical Technology Letters*, vol. 61, no. 2, pp. 425–430, 2018.

[15] Y. M. Pan, W. J. Yang, S. Y. Zheng, and P. F. Hu, "Design of wideband circularly polarized antenna using coupled rotated vertical metallic plates," *IEEE Transactions on Antennas and Propagation*, vol. 66, no. 1, pp. 42–49, 2018.

[16] G. Feng, L. Chen, X. Wang, and X. Xue, "Xiaowei Shi "Broadband circularly polarized crossed bowtie dipole antenna loaded with parasitic elements," *IEEE Antennas and Wireless Propagation Letters*, vol. 17, no. 1, pp. 1776–1779, 2018.

[17] W. J. Yang, Y. M. Pan, and S. Y. Zheng, "A low-profile wideband circularly polarized crossed-dipole antenna with wide axial-ratio and gain beamwidths," *IEEE Transactions on Antennas and Propagation*, vol. 66, no. 7, pp. 3346–3353, 2018.

[18] Z. Guo, Z. Zhao, and Y. Yang, "A directional circularly polarized crossed-dipole antenna with bandwidth enhancement," *Microwave and Optical Technology Letters*, vol. 60, no. 9, pp. 2161–2167, 2018.

[19] G. Feng, L. Chen, X. Xue, and X. Shi, "Broadband circularly polarized crossed-dipole antenna with a single asymmetrical cross-loop," *IEEE Antennas and Wireless Propagation Letters*, vol. 16, pp. 3184–3187, 2017.

[20] T. K. Nguyen and H. H. Tran, "A wideband dual-cavity-backed circularly polarized crossed dipole antenna," *IEEE Antennas and Wireless Propagation Letters*, vol. 16, pp. 3135–3138, 2017.

[21] L. Zhang, S. Gao, Q. Luo et al., "Single-feed ultra-wideband circularly polarized antenna with enhanced front-to-back ratio," *IEEE Transactions on Antennas and Propagation*, vol. 64, no. 1, pp. 355–360, 2016.

[22] R. Xu, J.-Y. Li, and W. Kun, "A broadband circularly polarized crossed-dipole antenna," *IEEE Transactions on Antennas and Propagation*, vol. 64, no. 10, pp. 4509–4513, 2016.

[23] S. X. Ta, "Crossed dipole loaded with magneto-electric dipole for wideband and wide-beam circularly polarized radiation," *IEEE Antennas and Wireless Propagation Letters*, vol. 14, pp. 358–361, 2015.